Range Resolution Improvement of a 24 GHz ISM Band Pulse Radar—A Feasibility Study

You-Sun Won, *Student Member, IEEE*, Chung-Hwan Kim, and Sang-Gug Lee, *Member, IEEE*

***Abstract*— An approach to improve the range resolution of a 24-GHz industrial, scientific, and medical (ISM) band pulse radar is presented for the automotive short-range radars. The resolution of the range profile was improved by applying the regularized least squares method to a discrete baseband signal at the receiver. For a 24-GHz ISM band pulse radar adopting a regularized least square method, a triangular pulse was identified as the optimal pulse shape under the regulations and in terms of cost effectiveness. To resolve multiple adjacent pulses with a constant false alarm rate, MATLAB simulations based on the least absolute shrinkage and selection operator (LASSO) algorithm were used to derive additional threshold values for output signals after the LASSO operation and the required signal-to-noise ratio (SNR). The simulated and measured values of the required SNR were 20.5 and 21.1 dB, respectively, for the two-target detection with a range resolution of 30 cm, at the detection and false alarm probabilities of 0.9 and 10^{-3}, respectively.**

***Index Terms*— Automotive radar, high range resolution, LASSO, narrowband pulse radar, regularized least squares.**

I. Introduction

As THE number of vehicles increases, the need for automotive safety systems also increases. Automotive safety systems can be grouped into two types: passive systems (such as adaptive air-bags and seatbelts) and active systems (such as dynamic control and collision avoidance systems). The probability of a collision can be significantly lowered when hazardous objects are sensed in advance, using active safety systems with radar sensors [1], [2]. However, active safety systems are usually available only in high-end vehicles due to the high cost of radar sensors [3]. In general, to detect objects in all directions around a vehicle, four or more short-range radar (SRR) sensors are required, while one long-range radar (LRR) sensor is needed to detect objects in the forward direction [4]. Lowering the cost of SRR sensors is an important requirement to achieve wider adoption of active safety systems.

Manuscript received July 1, 2015; accepted August 7, 2015. Date of publication August 17, 2015; date of current version October 15, 2015. This work was supported by the Information Technology Research and Development Program through the Ministry of Trade, Industry and Energy/Korea Evaluation Institute of Industrial Technology under Grant 10047107. The associate editor coordinating the review of this paper and approving it for publication was Dr. Lorenzo Lo Monte.

Y.-S. Won and S.-G. Lee are with the Korea Advanced Institute of Science and Technology, Daejeon 305-372, Korea (e-mail: yousun_won@kaist.ac.kr; sgjlee@kaist.ac.kr).

C.-H. Kim is with Wooriro Optical Telecom Company, Ltd., Gwangju 102-22, Korea (e-mail: forchiefclass@gmail.com).

Digital Object Identifier 10.1109/JSEN.2015.2469154

There are three frequency bands allocated for SRR: the 24 GHz industrial, scientific, and medical (ISM) band, ultra-wideband (UWB) band, and the 79 GHz UWB band. Since the semiconductor technologies that are used in 79 GHz radars are not yet cost effective, the 24 GHz bands are still more attractive [5]. The maximum detectable range can be enhanced by increasing the signal-to-noise ratio (SNR) through signal averaging, but this increases the range update time. Higher emission power reduces required signal averaging, and also allows the use of cheaper signal processors and a shorter update time. With 24 GHz UWB radar, even though the high range resolution of a few centimeters is available, a lot of averaging is required to meet the maximum detectable range of 30 m [3] due to the low peak emission power allowed. On the other hand, with 24 GHz ISM band radar, the allowed emission level is much higher, but its 200 MHz bandwidth significantly limits the range resolution. The range resolution of SRR for automotive safety applications has to be at least 30 cm to identify pedestrians in all directions [6]. However, with a 200 MHz bandwidth, the range resolution is 75 cm from the Rayleigh criterion [7], [8].

Many techniques to improve the range resolution beyond the Rayleigh criterion have been reported, such as super-resolution [8]–[10] and compressed sensing [11]–[13]. Most high resolution techniques enhance the range resolution by using various regression methods, including the regularized least squares (RLS) method [14]. One solution for a cost-effective and high range resolution SRR sensor would be to combine the proper regression method with a 24 GHz ISM band radar, thereby reducing averaging and improving range resolution. Although frequency modulated continuous wave (FMCW) radars are usually used for 24 GHz ISM band automotive applications due to their high SNR, pulse radars usually have lower hardware complexity and reduced calculation load for high resolution techniques than FMCW radars. Therefore, the present feasibility study on a 24 GHz ISM band radar with applied regression method was conducted using pulse radars.

In this paper, to improve the range resolution of 24 GHz ISM band pulse radar, the RLS method was applied to a discrete baseband signal at the receiver based on the least absolute shrinkage and selection operator (LASSO) algorithm [15], [16]. In addition to showing improved range resolution, the optimal pulse shape and additional detection threshold values for a constant false alarm rate (FAR) were

determined, and the required SNR for a range resolution of 30 cm was derived at a given FAR.

The remainder of this paper is organized as follows. Section II compares the estimated performance of automotive radars considering the regulations for frequency band selection. Section III analyzes and explains considerations when applying the RLS method to a 24 GHz ISM band pulse radar. Section IV presents simulation results of a 24 GHz ISM band pulse radar adopting the LASSO algorithm, and Section V presents conclusions.

II. Frequency Band Selection for SRR Sensors

Among the important parameters that affect radar performance such as range resolution and maximum detectable range, the bandwidth and peak power of the transmit signal are dominant. From the Rayleigh criterion, it is possible to distinguish two echo signals that are separated by more than half of the signal pulse width [8]. Therefore, the range resolution ΔR can be given by [17]

$$\Delta R = \frac{c \cdot T_{PW}}{2} = \frac{c}{2B} \tag{1}$$

where c is the speed of light, T_{PW} is the signal pulse width, and B is the signal bandwidth. Equation (1) shows that a narrower pulse width due to a wider signal bandwidth allows better range resolution.

On the other hand, the maximum detectable range $R_{\max}$ is given by [17]

$$R_{\max} = \left[\frac{\mathrm{EIRP_{pk}} \cdot G_{RX} \cdot \lambda^2 \cdot \sigma \cdot G_{avg}}{(4\pi)^3 kTBF\,(\mathrm{SNR_{min}})} \right]^{\frac{1}{4}} \tag{2}$$

where $\mathrm{EIRP_{pk}}$ is the peak effective isotropically radiated power, G_{RX} is the receiver antenna gain, λ is the signal wavelength in air, σ is the target cross-section, G_{avg} is the processing gain obtained by averaging, kT is the thermal noise per hertz, F is the receiver noise factor, and $\mathrm{SNR_{min}}$ is the minimum required SNR. The $\mathrm{SNR_{min}}$ can be calculated from the specified probabilities of detection (P_D) and false alarm (P_{FA}) based on the detection theory [17]. In general, the wavelength, bandwidth, and peak power of the transmit signal are given by regulations, whereas the receiver noise factor, antenna gain, target cross-section, P_D, and P_{FA} are set to satisfy the system requirements. Therefore, when the operating frequency band and system requirements are given, the single-shot detectable range can be estimated from (2) by setting $G_{avg} = 1$, or the required G_{avg} for the targeted maximum detectable range can also be found from (2). A typical automotive SRR sensor requires P_D and P_{FA} values of 0.9 and 10^{-3}, respectively, which correspond to the $\mathrm{SNR_{min}}$ of 11 dB [4].

The maximum detectable range can be effectively improved through pulse compression [17]. Pulse compression enables the transmit signal energy to be increased without decreasing the range resolution by using a long transmit pulse that consists of coded short-pulse trains. For pulse compression, a matched filter correlates received signals with delayed versions of the transmitted waveform. However, the matched filter often suffers from sidelobes masking echo signals from nearby targets [18]. Other pulse compression methods, such as mismatched filtering and least squares estimation, have been reported to reduce the range sidelobes [18]–[20]. By applying the least mean squares (LMS) method to the envelope of an oversampled signal in the range domain, a range profile with an improved range resolution can be obtained [21], [22]. To adopt the LMS method in the range domain, each echo signal has to be received without matched filtering and converted to a discrete signal by an analog-to-digital converter (ADC). An insufficient SNR problem due to the digitization of each non-compressed pulse can be solved by averaging successive received pulses. To increase the SNR and thus increase the maximum detectable range, only the averaging technique is discussed here.

TABLE I
Radar Performance Estimation

	24 GHz UWB		24 GHz ISM	
Country	EU	USA	EU	USA
Bandwidth (GHz)	4	7	0.2	0.25
Peak EIRP (dBm)	2.02	4.45	20	12.7
Range resolution (cm)	3.75	2	75	60
$\mathrm{SNR_{min}}$ (dB)	11			
Single-shot detectable range (m)	1.37	1.78	9.40	5.83
Coherent averaging number[a]	226,669	80,318	104	699

NF=5 dB, antenna gain=15 dBi, RCS=1m^2, P_D=0.9, and P_{FA}=10^{-3}
[a]To meet the required maximum detectable range of 30 m

To select a suitable operating frequency band for automotive SRR sensors, radar performance parameters have to be estimated for the allocated bands. For automotive SRR sensors, the European Telecommunications Standards Institute (ETSI) has allocatedthe 24 GHz ISM and UWB bands as well as the 79 GHz UWB band, whereas the Federal Communication Commission (FCC) has allocated the 24 GHz ISM and UWB bands [4], [5]. In the 24 GHz UWB band, the peak EIRP is -34 dBm/MHz [23] with bandwidths of 4 and 7 GHz, whereas in the ISM band, the peak EIRP is 20 and 12.7 dBm with bandwidths of 200 and 250 MHz, as stipulated by ETSI and FCC standards, respectively. In the 79 GHz UWB band, the peak EIRP of 55 dBm with a bandwidth of 4 GHz is standardized by ETSI. Considering the cost advantage of the 24 GHz radar compared with 79 GHz due to semiconductor technology costs, 24 GHz radar was selected, and a performance comparison between 24 GHz radars considering the regulations is shown in Table I.

Assuming the system noise figure (NF) of 5 dB, antenna gain of 15 dBi, radar cross section (RCS) of 1 m^2, P_D of 0.9, and P_{FA} of 10^{-3}, the range resolution and single-shot detectable range of the radar can be calculated by (1) and (2), respectively. The number of coherent averaging operations that meets the typical maximum detectable range of 30 m can also be found by (2). Table I shows that, with the UWB radar, although the range resolution is very high, large averaging numbers of 226,669 or 80,318 are required to detect targets up to 30 m. On the other hand, much less coherent averaging is required for the ISM band radar. However, with the ISM band radar, the range resolution is more limited, since its signal bandwidth is narrower than that of the UWB radar.

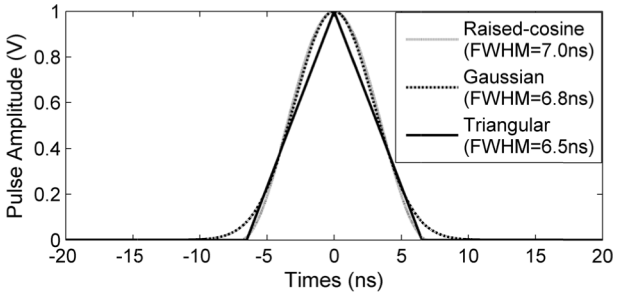

Fig. 1. Normalized baseband pulse candidates satisfying OBW of 100 MHz (raised cosine, Gaussian, and triangular pulses).

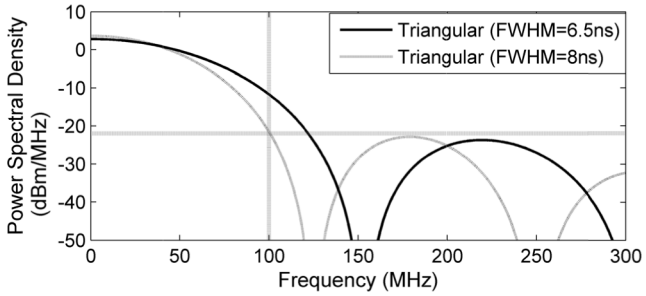

Fig. 2. Peak power spectral density of triangular pulses (FWHM = 6.5 and 8 ns) with the peak EIRP of 20 dBm.

In the ISM band pulse radar, it is difficult to distinguish each pulse signal when several long pulse signals are overlapped. However, a high-resolution range-profile can be constructed from a received signal based on the regression method using a transmitted pulse waveform, and in that case each echo signal coming from targets becomes distinguishable. Therefore, a 24 GHz ISM band pulse radar which adopts the RLS method, a regression method, can provide improved range resolution, while requiring less averaging due to high EIRP.

III. Implementation Issues of 24 GHz Narrowband Pulse Radar Adopting the RLS Method

A. Design of Baseband Pulse

To implement a pulse radar that operates in the 24 GHz ISM band, the pulse shape, amplitude, and width of the baseband transmit pulse signal have to be optimized considering the regulations and other important factors, such as the full-width at half-maximum (FWHM) of the pulse and the hardware complexity for pulse generation. To design a transmit pulse signal, only the ETSI standard [24] is considered because the pulse signal tailored to the ETSI standard can be applied to the FCC standard allowing a shorter pulse width. In the ETSI standard, when the baseband pulse signal is unipolar, the symmetric spectral nature of the transmitted pulse requires an occupied bandwidth (OBW) of 100 MHz. The OBW must contain more than 99% of the pulse power. The peak amplitude of the transmit signal is limited to meet the peak EIRP of 20 dBm. The unwanted (out-of-band) emission must be less than −30 dBm/MHz, and it can be met by reducing the pulse repetition frequency (PRF).

Fig. 1 shows the normalized baseband pulse candidates, namely, the raised cosine, Gaussian, and triangular pulses with the pulse widths needed to meet the OBW of 100 MHz. As shown in Fig. 1, the raised-cosine pulse has the longest FWHM (7.0 ns), whereas the triangular pulse has the smallest FWHM (6.5 ns). In addition to the advantage of the small FWHM, the triangular pulse can be easily generated by a charge pump circuit. Therefore, the triangular pulse was selected as the optimal pulse shape.

Fig. 2 shows the peak power spectral densities (PSD) of triangular pulses (FWHM=6.5 and 8 ns) with the peak EIRP of 20 dBm. To get some margin in the OBW and for a lower unwanted emission level, the FWHM of the triangular pulse in Fig. 1 (6.5 ns) was increased to 8 ns. As shown in Fig. 2, with a FWHM of 8 ns (pulse width of 16 ns), the peak unwanted emission level is −22.0 dBm/MHz which is the peak value of the first side-lobe. With the same peak unwanted emission level, the FWHMs of the raised-cosine, Gaussian, and triangular pulses are 9.1 ns, 9.3 ns and 8.0 ns, respectively, confirming that the triangular pulse still has the smallest FWHM. To meet the unwanted emission level of −30 dBm/MHz, the average power can be controlled by lowering the PRF based on the equation given by [17]

$$P_{avg} = P_{peak} + 20\log\left(T_{PW} \cdot \mathrm{PRF}\right) \tag{3}$$

where P_{avg} is the average power, P_{peak} is the peak power, and T_{PW} is the pulse width. From (3), when the peak power and pulse width are −22.0 dBm/MHz and 16 ns, respectively, the average power becomes −30 dBm/MHz with a PRF of 24.9 MHz, which is larger than the maximum PRF of 5 MHz to provide an unambiguous range of 30 m. Therefore, the average power of unwanted emission can be made lower than −30 dBm/MHz.

B. Discrete Baseband Signal at the Receiver

To obtain a baseband signal at the receiver, which is an echo signal reflected from targets, two methods were utilized: signal generation by MATLAB and measurement using a radar module. Fig. 3 shows examples of generated and measured echo signals from two targets with a range spacing of 30 cm at the SNR of 20 dB. An echo signal generated by MATLAB simulation is shown in Fig. 3 (a). To generate an echo signal, a triangular pulse with the pulse width of 16 ns and point scatterers were used as a transmit signal and test targets, respectively. For convenience, an ideal echo signal was generated from the given target positions without considering the path loss, and Gaussian random noise was summed to an ideal echo signal depending on given SNRs.

Fig. 3 (b) shows echo signals obtained through the measurement of the radar module. In order to get an actual echo signal, a 24 GHz ISM band pulse radar was implemented using commercial chips and 0.13-μm CMOS integrated circuits (ICs). Fig. 4 shows the block diagram and photograph of the ISM band pulse radar module. As shown in Fig. 4 (a), a transmitter (Tx), which consists of a pulse generator, an up-conversion mixer [25], a power amplifier (PA), and an antenna, generates and emits a triangular pulse signal with a pulse width and center frequency of 16 ns and 24.125 GHz,

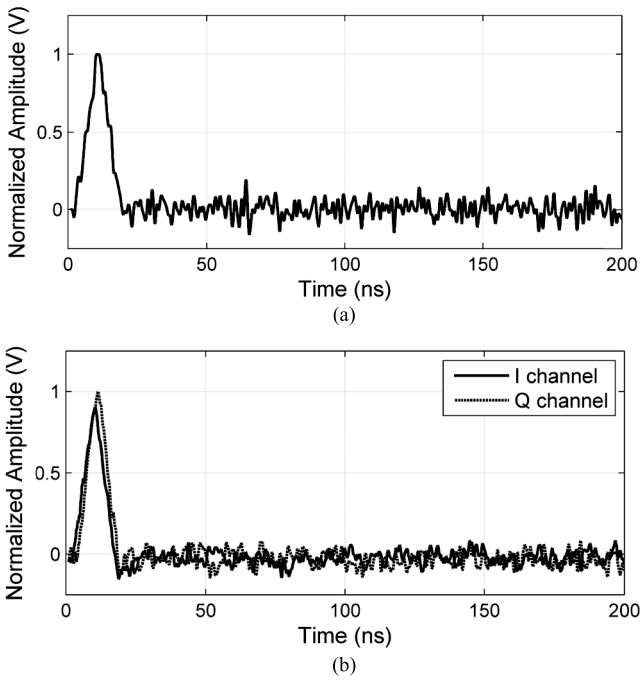

Fig. 3. Examples of echo signals from two targets with the range spacing of 30 cm at the SNR of 20 dB. (a) Generated echo signal by MATLAB simulation. (b) Measured echo signals from a radar module.

respectively, whereas a receiver (Rx), which consists of an antenna, a low noise amplifier (LNA), a down-conversion mixer, and a programmable gain amplifier (PGA), amplifies and outputs a down-converted echo signal. A 24 GHz LO signal is generated and divided by a voltage controlled oscillator (VCO)/phase-locked loop (PLL) and a power splitter, respectively. The PRF is determined by a switching signal from a clock generator. Fig. 4 (b) shows the implemented 24 GHz ISM band pulse radar module. The measured pulse width and amplitude of the triangular pulse are 16.0 ns and 577.0 mV_{pp}, respectively. With a 5 MHz PRF, the measured average power of the emitted pulse is -25.9 dBm, and the OBW of the triangular pulse is 160.2 MHz, thus satisfying the regulations. Two trihedral corner reflectors were used as test targets, and measurements were conducted in a radio anechoic chamber to avoid clutter signals. Baseband echo signals at the receiver output were measured by an oscilloscope and processed by MATLAB simulation. The averaging number was set to meet a given SNR.

To adopt the RLS method, a baseband echo signal needs to be converted to a discrete signal by an ADC. The sampling rate of the ADC has to be greater than twice the maximum signal bandwidth based on the Nyquist rate. The desired range resolution for SRR applications is 30 cm or less [6], requiring a bandwidth of 500 MHz based on (1). Therefore, the sampling rate is determined by the desired bandwidth of 500 MHz to obtain a precise envelope of an echo signal without using an interpolation filter, even though the signal bandwidth of the ISM band radar is 200 MHz. Overlapped echo signals from adjacent targets can be decomposed using a transmit template signal by applying the RLS method to an oversampled signal in the range domain, and thus the range resolution can be improved [21], [22]. In this study, a 1 GS/s 6-bit ADC was

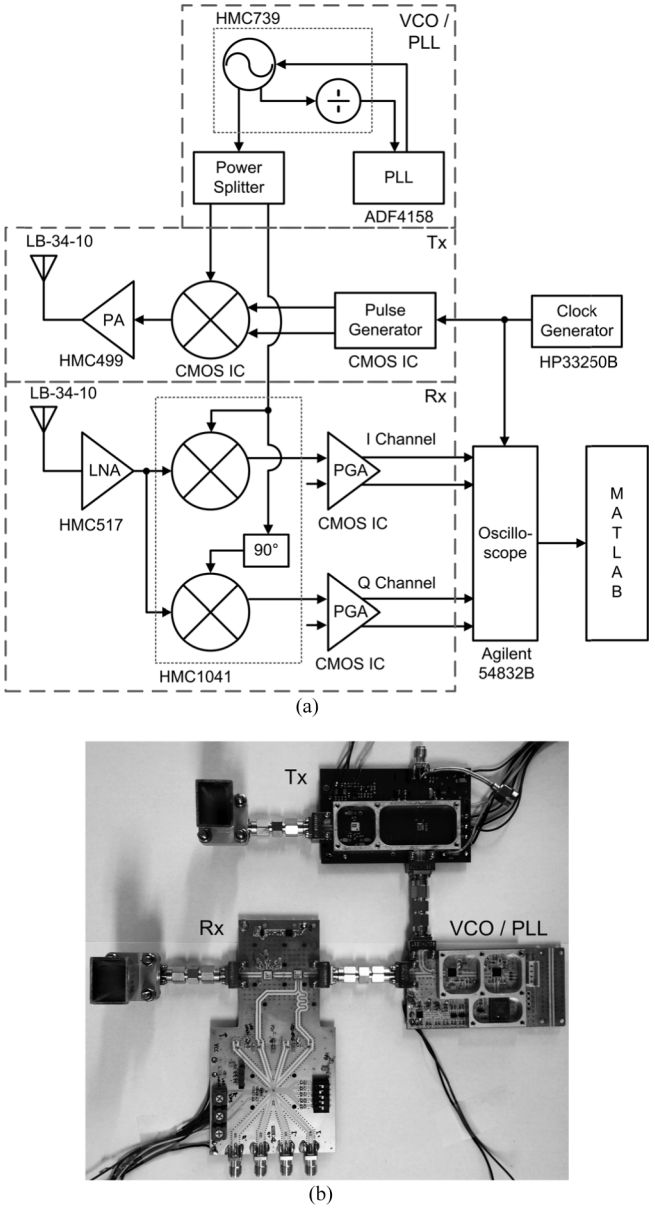

Fig. 4. 24 GHz ISM band pulse radar module. (a) Block diagram. (b) Photograph.

chosen to achieve a discrete baseband signal. Noting that various CMOS flash ADCs that provide the sampling rate of more than 10 GHz have been reported recently [26], the ADC can be developed by medium-level CMOS technologies.

C. Regularized Least Squares Methods

The LMS method can be utilized to solve the discrete linear equations defined as

$$\mathbf{y} = \mathbf{D}\mathbf{x} = \begin{bmatrix} s_1 & 0 & \cdots & 0 \\ \vdots & s_1 & & \vdots \\ s_L & \vdots & \ddots & 0 \\ 0 & s_L & & s_1 \\ \vdots & & \ddots & \vdots \\ 0 & \cdots & 0 & s_L \end{bmatrix} \begin{bmatrix} x_1 \\ x_2 \\ x_3 \\ \vdots \\ x_{M-1} \\ x_M \end{bmatrix} \tag{4}$$

where $\mathbf{y}$ is the measured echo signal at the baseband in the discrete time domain, $\mathbf{D}$ is the correlation matrix, and $\mathbf{x}$ is the estimated discrete range vector. The range profile $\mathbf{x}$ contains the amplitude of the reflected signal at the position index where the reflection occurs. In (4), the correlation matrix $\mathbf{D}$ is parameterized by the columns of the discrete range-shifted versions of the normalized transmit pulse signal $\mathbf{s} = [s_1\ s_2\ \cdots s_L]^T$ having a discrete and fixed range-width of an integer L. Since $\mathbf{y}$ and $\mathbf{D}$ are known in (4), $\mathbf{x}$ can be found by minimizing the mean-squared error given by [14]

$$\arg\min_{\mathbf{x}} \|\mathbf{D}\mathbf{x} - \mathbf{y}\|_2^2 . \tag{5}$$

However, when the measured signal $\mathbf{y}$ is noisy, some non-zero components in $\mathbf{x}$ can occur to fit the noisy signal, which is called overfitting. Therefore, to suppress overfitting as much as possible, the sparse estimation of $\mathbf{x}$ is desirable. Sparse non-zero components of $\mathbf{x}$ mean that few non-zero components of $\mathbf{x}$ due to noise occur.

To reduce the non-zero components in $\mathbf{x}$, the l_{p}-regularization, a regularized form of (5), can be adopted and given by [14]

$$\arg\min_{\mathbf{x}} \left\{ \|\mathbf{D}\mathbf{x} - \mathbf{y}\|_2^2 + \alpha \|\mathbf{x}\|_p \right\}, \tag{6}$$

$$\|\mathbf{x}\|_p = \begin{cases} \left(\sum_{i=0}^{n} |\mathbf{x}_i|^p \right)^{1/p}, & p \geq 1 \\ \sum_{i=0}^{n} |\mathbf{x}_i|^p, & 0 < p < 1 \\ \sum_{i=0}^{n} 1_{\mathbf{x}_i \neq 0}, & p = 0 \end{cases} \tag{7}$$

where $\|\mathbf{x}\|_p$ is the l_{p}-norm, and α is the regularization parameter. The l_0-, l_1-, and l_2-norms mean the number of non-zero components, the sum of the absolute values, and the Euclidean length of $\mathbf{x}$, respectively. The l_0-regularization finds the sparsest solution of $\mathbf{x}$ by minimizing the l_0-norm. However, it is difficult to find the correct solution of the l_0-regularization, because the number of all cases of $\mathbf{x}$ has to be checked. From the l_2-regularization, a closed-form solution can be achieved by minimizing the l_2-norm, but it is not sparse enough. On the other hand, by the l_1-regularization, the sparsest solution can be obtained with a proper regularization parameter.

Fig. 5 shows simulated P_D and P_{FA} when two targets are located with a range spacing of 30 cm. To find a proper algorithm for a 24 GHz ISM band pulse radar, four well-known algorithms, the conjugate gradient method (CGM) [27], In-Crowd [28], LASSO, and least square with QR factorization (LSQR) [29], were applied to echo signals that were generated by MATLAB, as shown in Fig. 3 (a). Conventional detection threshold values were determined for P_{FA} of 10^{-3} based on the detection theory by assuming that the noise has a Gaussian distribution [17], [30]. After applying each algorithm, non-zero components occur, and a decision of detection or false alarm is made by positions of non-zero components which exceed the detection threshold. As shown in Fig. 5 (a) and (b), when the LASSO algorithm is applied, a more accurate range profile can be obtained,

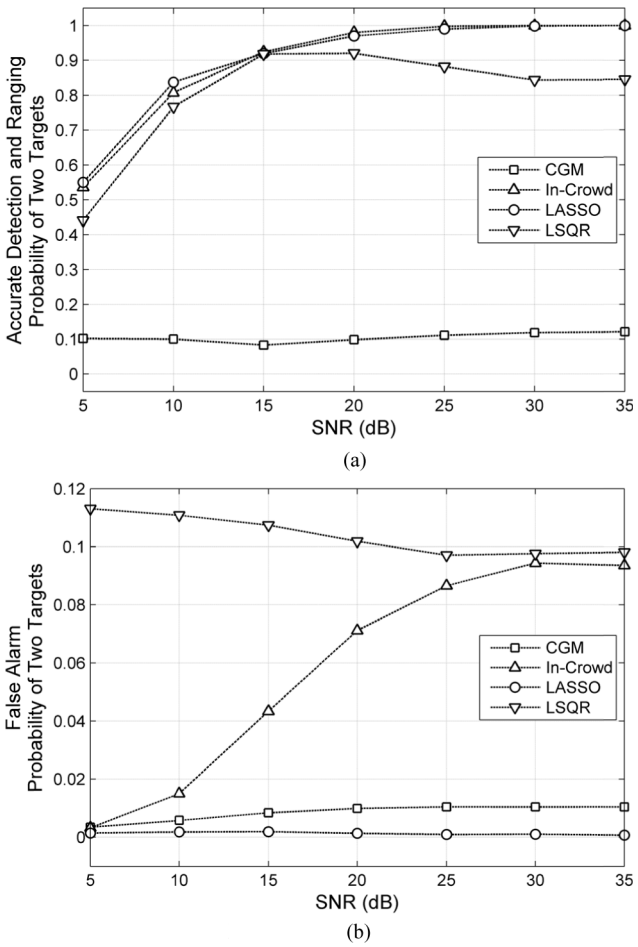

Fig. 5. Simulated P_D and P_{FA} for detecting two targets with the range spacing of 30 cm. (a) Probability of detection. (b) Probability of false alarm.

while suppressing non-zero components caused by noise (false alarm). LASSO [15], [16] is one of the algorithms capable of finding the l_1-regularization solution in a short time. Therefore, to improve the range resolution of the ISM band pulse radar, the LASSO algorithm was chosen to implement the RLS method by applying it to a discrete baseband signal at the radar receiver.

D. Additional Detection Threshold for LASSO Outputs

Fig. 6 shows the dual detection thresholds (first and second thresholds) values at each P_{FA} and the SNR. In the conventional detection method, in order not to exceed a given FAR, a detection threshold, called the first threshold, is determined uniquely from the noise probability density function [17]. However, after the LASSO operation, false non-zero components in $\mathbf{x}$ can be generated due to noise and signal distortion. Therefore, to sustain the required FAR, an additional detection threshold, called the second threshold, is introduced to reject the incorrect components of $\mathbf{x}$. By adopting the second threshold after the LASSO simulation, the FAR can be reduced significantly because at moderate or high SNRs, most false alarm signals have smaller amplitudes than real pulse signals. Note that the first threshold is used in the LASSO simulation to select non-zero components

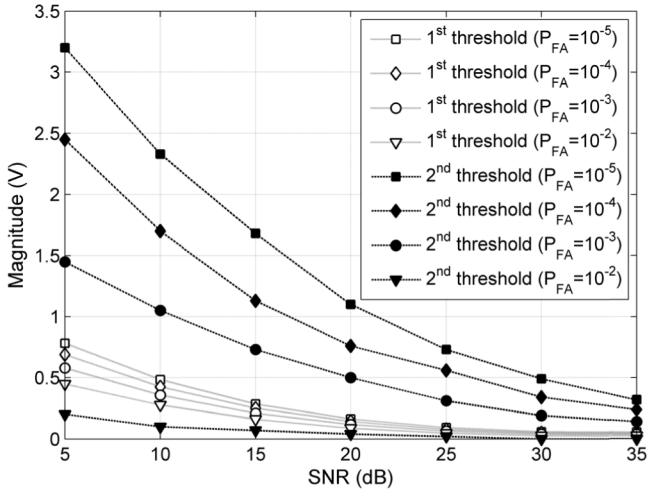

Fig. 6. Dual detection thresholds (first and second thresholds) values.

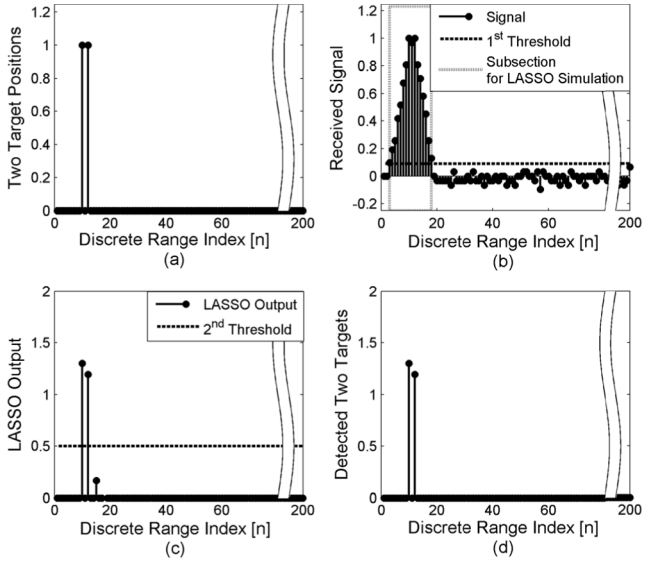

Fig. 7. Simulation processes in discrete time domain: (a) initial position of two targets, (b) received signal y with noise, (c) result of LASSO simulation in **x**, and (d) two successfully detected targets in **x**.

in submatrix **D** and subsection **x**, where the intervals in **y** exceed the threshold from (6), and this effectively reduces calculation load. The second threshold values are found from the output data of the LASSO simulation to meet a given FAR. The LASSO simulation was performed ten million times for two equal amplitude pulses spaced with a range distance ΔR at each SNR. Here, ΔR was changed from 30 cm to 75 cm with a minimum range step of 15 cm, which corresponds to a 1 ns round-trip time. The threshold values in Fig. 6 were used in the following simulation.

E. Range Update Time

The short-range update time is an important factor for automotive radar. To determine the effect of the regression methods on the range update time, the computational complexity of the regression methods has to be considered. When **D** is an M×M matrix and **y** is an M×1 vector in (6), the LASSO algorithm has a computational complexity of $O(\mathrm{M}^3)$ [16]. However, as mentioned earlier, because the LASSO algorithm operates only with the range bins that are over the first detection threshold, the computational complexity can be much lower than $O(\mathrm{M}^3)$. For example, assuming that one-third of the entire range exceeds the first detection threshold, the computational complexity is reduced to one twenty-seventh of $O(\mathrm{M}^3)$. Assuming that 10% of **y** entries exceed the first detection threshold when two targets exist with a maximum range of 30 m, requiring a 200×200 matrix **D**, a 20×20 sub-matrix in **D** and a 20×1 sub-vector in **y** will be used for the LASSO algorithm. Using a low-end DSP of TMS320F28335, the LASSO operation for detecting two targets is expected to take an average calculation time of 0.8 ms. With the DSP, it takes 0.1 μs to perform single floating point multiplication. Neglecting data acquisition time, 0.8 ms corresponds to a range update frequency of about 1.25 kHz, which is an acceptable value for automotive applications, and the range update frequency can be increased further with a high-end DSP or dedicated field programmable gate array (FPGA) ICs.

IV. Simulation Results

As discussed earlier, the RLS method was implemented to improve range resolution by applying the LASSO simulation to a discrete baseband signal at a radar receiver using the first and second threshold values. Also, as previously mentioned, a triangular pulse with a pulse width of 16 ns was utilized as a baseband pulse signal. The generated or measured signals shown in Fig. 3 were used as the echo pulse signal **y** in (6). Fig. 7 shows the MATLAB simulation processes in the discrete range domain used to construct a range profile which has a higher range resolution. Since the unit discrete range index corresponds to 15 cm, the maximum range index of 200 corresponds to a 30 m range. As shown in Fig. 7 (a), the positions of two targets are given in the discrete range domain. An example of a received signal **y** from two targets at an SNR of 20 dB is shown in Fig. 7 (b). As mentioned earlier, the first threshold (conventional detection threshold) is used to select the non-zero subsection of **x**, where the intervals in **y** exceed the threshold value. In (6), with the LASSO algorithm [15], the regularized parameter a is set by $\sum_{i=1}^{n} 2|\mathbf{D}' \cdot (\mathbf{y} - \mathbf{D} \cdot \mathbf{x}_0)|_i / n$, where $\mathbf{x}_0$ is initial **x**. After the LASSO simulation with the subsection of **x**, LASSO outputs of more than two non-zero bins are shown in Fig. 7 (c). Applying the second threshold in Fig. 6, two targets were successfully detected as shown in Fig. 7 (d).

Fig. 8 shows the probabilities of exactly detecting two targets within the range accuracy of ±15 cm at $P_{FA} = 10^{-3}$. Based on Fig. 8, to resolve two targets separated by 30 cm at the P_D of 0.9, the required $\mathrm{SNR}_{\mathrm{min}}$ are 20.5 and 21.1 dB for the simulated (generated) and measured echo signals, respectively, which are 9.5 and 10.1 dB higher than that required for conventional single-target detection, respectively. In other words, for $P_{FA} = 10^{-3}$ and P_D of 0.9, the $\mathrm{SNR}_{\mathrm{min}}$ of 11 dB is required only to discriminate the existence of echo signals regardless of target numbers [17],

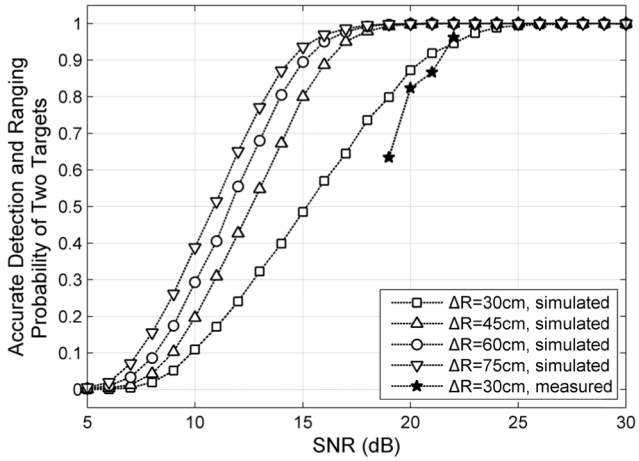

Fig. 8. Accurate detection and ranging probabilities of two targets at $P_{FA} = 10^{-3}$.

whereas the SNR_{min} of 21.1 dB is required to exactly identify two targets with the range resolution of 30 cm. Thus, successful detection for the multi-target condition requires both the exact coincidence of target numbers and the satisfaction of the specified range accuracy and resolution, resulting in a higher required SNR_{min}. To satisfy the SNR of 21.1 dB, the coherent averaging number of 1,066 is required, which is still much lower than that of the UWB radar shown in Table I.

The proposed radar shows better range resolution than the typical ISM band radar and much less averaging than the UWB radar. Therefore, the proposed pulse radar can be a good candidate for cost-effective SRR sensor applications.

V. Conclusion

The application of SRR in the 24 GHz ISM band has been limited, due to the narrow bandwidth which results in a low range resolution of 75 cm. To improve the range resolution, this paper proposed a narrowband pulsed radar which adopts the RLS method based on the LASSO algorithm. A triangular pulse with a pulse width of 16 ns was utilized as a transmit baseband signal to satisfy the ETSI regulation. To implement the RLS method, LASSO simulation with dual detection thresholds was applied to a received baseband signal. Using the proposed method, the typical range resolution of 75 cm can be improved to 30 cm with simulated and measured values of SNR_{min} of 20.5 and 21.1 dB, respectively, for $P_{FA} = 10^{-3}$ and P_D of 0.9. The acceptable coherent averaging number with the improved range resolution compensates the SNR penalty and makes the radar proposed here a good candidate for SRR applications. The proposed method also predicts the probabilities of target detection and false alarm within the specified range resolution and accuracy.

References

[1] J. Wenger, "Automotive radar—Status and perspectives," in *Proc. IEEE Compound Semiconductor Integr. Circuit Symp.*, Oct./Nov. 2005, pp. 21–24.

[2] A. Etinger, N. Balal, B. Litvak, M. Einat, B. Kapilevich, and Y. Pinhasi, "Non-imaging MM-wave FMCW sensor for pedestrian detection," *IEEE Sensors J.*, vol. 14, no. 4, pp. 1232–1237, Apr. 2013.

[3] J. Hasch, E. Topak, R. Schnabel, T. Zwick, R. Weigel, and C. Waldschmidt, "Millimeter-wave technology for automotive radar sensors in the 77 GHz frequency band," *IEEE Trans. Microw. Theory Techn.*, vol. 60, no. 3, pp. 845–860, Mar. 2012.

[4] I. Gresham *et al.*, "Ultra-wideband radar sensors for short-range vehicular applications," *IEEE Trans. Microw. Theory Techn.*, vol. 52, no. 9, pp. 2105–2122, Sep. 2004.

[5] V. Jain, F. Tzeng, L. Zhou, and P. Heydari, "A single-chip dual-band 22–29-GHz/77–81-GHz BiCMOS transceiver for automotive radars," *IEEE J. Solid-State Circuits*, vol. 44, no. 12, pp. 3469–3485, Dec. 2009.

[6] European Telecommunications Standards Institute, "Electromagnetic compatibility and radio spectrum matters (ERM); SRD radar equipment using wideband low activity mode (WLAM) and operating in the frequency range from 24,05 GHz to 24,50 GHz; system reference document," Eur. Telecommun. Standards Inst., Sophia Antipolis, France, Tech. Rep. ETSI TR 102-892, 2011.

[7] A. Blanco-del-Campo, A. Asensio-López, J. Gismero-Menoyo, B. P. Dorta-Naranjo, and J. Carretero-Moya, "Instrumental CWLFM high-range resolution radar in millimeter waveband for ISAR imaging," *IEEE Sensors J.*, vol. 11, no. 2, pp. 418–429, Feb. 2011.

[8] P. Tait, *Introduction to Radar Target Recognition*. Stevenage, U.K.: The Institution of Engineering and Technology, 2005.

[9] S. Liu and J. Xiang, "Novel method for super-resolution in radar range domain," *IEE Proc. Radar, Sonar, Navigat.*, vol. 146, no. 1, pp. 40–44, Feb. 1999.

[10] S. D. Blunt, K. Gerlach, and T. Higgins, "Aspects of radar range super-resolution," in *Proc. IEEE Radar Conf.*, Apr. 2007, pp. 683–687.

[11] G. Shi, J. Lin, X. Chen, F. Qi, D. Liu, and L. Zhang, "UWB echo signal detection with ultra-low rate sampling based on compressed sensing," *IEEE Trans. Circuits Syst. II, Exp. Briefs*, vol. 55, no. 4, pp. 379–383, Apr. 2008.

[12] M. A. Herman and T. Strohmer, "High-resolution radar via compressed sensing," *IEEE Trans. Signal Process.*, vol. 57, no. 6, pp. 2275–2284, Jun. 2009.

[13] Z. Liu, X. Wei, and X. Li, "Aliasing-free moving target detection in random pulse repetition interval radar based on compressed sensing," *IEEE Sensors J.*, vol. 13, no. 7, pp. 2523–2534, Jul. 2013.

[14] M. Ndoye and J. M. M. Anderson, "An MM-based algorithm for L1-regularized least squares estimation in GPR image reconstruction," in *Proc. IEEE Radar Conf.*, Apr./May 2013, pp. 1–6.

[15] K. Sjöstrand, L. H. Clemmensen, R. Larsen, and B. Ersbøll, "Spasm: A MATLAB toolbox for sparse statistical modeling," Tech. Univ. Denmark, Lyngby, Denmark. [Online]. Available: http://www2.imm.dtu.dk/projects/spasm/references/spasm.pdf.

[16] S. Rosset and J. Zhu, "Piecewise linear regularized solution paths," *Ann. Statist.*, vol. 35, no. 3 pp. 1012–1030, Jun. 2007.

[17] M. I. Skolnik, *Introduction to Radar Systems*, 2nd ed. New York, NY, USA: McGraw-Hill, 1980.

[18] S. D. Blunt and K. Gerlach, "Adaptive pulse compression via MMSE estimation," *IEEE Trans. Aerosp. Electron. Syst.*, vol. 42, no. 2, pp. 572–584, Apr. 2006.

[19] J. E. Cilliers and J. C. Smit, "Pulse compression sidelobe reduction by minimization of L_p-norms," *IEEE Trans. Aerosp. Electron. Syst.*, vol. 43, no. 3, pp. 1238–1247, Jul. 2007.

[20] A. B. Yoldemir and M. Sezgin, "A least squares approach to buried object detection using ground penetrating radar," *IEEE Sensors J.*, vol. 11, no. 6, pp. 1337–1341, Jun. 2011.

[21] I. S. Simić, A. J. Zejak, Z. T. Golubičić, and A. Petrović, "Improved radar range resolution achieved by mismatched filter," in *Proc. IEEE Medit. Electrotech. Conf.*, vol. 1. May 1998, pp. 435–438.

[22] T.-Y. Yu, G. Zhang, A. B. Chalamalasetti, R. J. Doviak, and D. Zrníc, "Resolution enhancement technique using range oversampling," *J. Atmos. Ocean. Technol.*, vol. 23, no. 2, pp. 228–240, Feb. 2006.

[23] European Telecommunications Standards Institute, "Electromagnetic compatibility and radio spectrum matters (ERM); short range devices; road transport and traffic telematics (RTTT); short range radar equipment operating in the 24 GHz range; part 1: Technical requirements and methods of measurement," Eur. Telecommun. Standards Inst., Tech. Rep. ETSI EN 302-288-1, 2006.

[24] European Telecommunications Standards Institute, "Electromagnetic compatibility and radio spectrum matters (ERM); road transport and traffic telematics (RTTT); short range radar equipment operating in the 24,05 GHz to 24,25 GHz frequency range for automotive application; part 2: Harmonized EN covering the essential requirements of article 3.2 of the R&TTE directive," Eur. Telecommun. Standards Inst., Tech. Rep. ETSI EN 302-858-2, 2011.

[25] Y.-S. Won, C.-H. Kim, and S.-G. Lee, "A 24 GHz highly linear up-conversion mixer in CMOS 0.13 μm technology," *IEEE Microw. Compon. Lett.*, vol. 25, no. 6, pp. 400–402, Jun. 2015.
[26] S. Verma *et al.*, "A 10.3 GS/s 6b flash ADC for 10 G Ethernet applications," in *IEEE Int. Solid-State Circuits Conf. Dig. Tech. Papers (ISSCC)*, vol. 1. Feb. 2013, pp. 462–463.
[27] M. Lustig, D. L. Donoho, and J. M. Pauly, "Sparse MRI: The application of compressed sensing for rapid MR imaging," *Magn. Reson. Med.*, vol. 58, no. 6, pp. 1182–1195, 2007.
[28] P. R. Gill, A. Wang, and A. Molnar, "The in-crowd algorithm for fast basis pursuit denoising," *IEEE Trans. Signal Process.*, vol. 59, no. 10, pp. 4595–4605, Oct. 2011.
[29] C. C. Paige and M. A. Saunders, "LSQR: An algorithm for sparse linear equations and sparse least squares," *ACM Trans. Math. Softw.*, vol. 8, no. 1, pp. 43–71, 1982.
[30] W. J. Dixon and F. J. Massey, Jr., *Introduction to Statistical Analysis*, 3rd ed. New York, NY, USA: McGraw-Hill, 1969, pp. 52–54.

You-Sun Won received the B.S. degree in information and communication engineering from Ewha Womans University, Seoul, Korea, in 2009, and the M.S. degree in electrical engineering from the Korea Advanced Institute of Science and Technology, Daejeon, Korea, in 2011, where she is currently pursuing the Ph.D. degree in electrical engineering. Her research interests include microwave filter and RF-IC designs for wireless and radar transceivers, and radar system designs.

Chung-Hwan Kim received the B.S., M.S., and Ph.D. degrees in semiconductor physics from Seoul National University, Korea, in 1985, 1987 and 1993, respectively. From 1993 to 2000, he was with ETRI, as a Senior Engineering Staff, where he was involved in the design and testing of the RF IC's in wireless communications using compound semiconductor and CMOS technologies. From 2000 to 2011, he was one of the co-founders of a venture company, Teltron Inc. He is currently with Wooriro Optical Telecom Company, Ltd., where he is also a Managing Director, responsible for the development of range-finding systems including LADAR and Radar.

Sang-Gug Lee received the B.S. degree in electronic engineering from Kyungpook National University, Korea, in 1981, and the M.S. and Ph.D. degrees in electrical engineering from the University of Florida, Gainesville, in 1989 and 1992, respectively. In 1992, he joined Harris Semiconductor, Melbourne, FL, USA, where he was engaged in silicon-based RFIC designs. From 1995 to 1998, he was an Assistant Professor with the School of Computer and Electrical Engineering, Handong University, Pohang, Korea. From 1998 to 2009, he was with Information and Communications University, Daejeon, Korea, and became a Full Professor. Since 2009, he has been with the Korea Advanced Institute of Science and Technology, Daejeon, where he has been a Professor with the Department of Electrical Engineering. His research interests include CMOS-based RF, analog, and mixed mode IC designs for various radio transceivers, especially the ultralow power applications. His research interests extend to extreme high-frequency (THz) circuit designs, display semiconductors, and energy-harvesting IC designs.